Heat-shock protein 60 is required for blastema formation and maintenance during regeneration

Shinji Makino*†, Geoffrey G. Whitehead*, Ching-Ling Lien*, Soo Kim*, Payal Jhawar*, Akane Kono‡, Yasushi Kawata‡, and Mark T. Keating*†

*Howard Hughes Medical Institute, Department of Cardiology, Children's Hospital, and Departments of Pediatrics and Cell Biology, Harvard Medical School, Boston, MA 02115; and ‡Department of Biotechnology, Faculty of Engineering, and Department of Biomedical Science, Institute of Regenerative Medicine and Biofunction, Graduate School of Medical Science, Tottori University, Koyama-Minami, Tottori 680-8552, Japan

Contributed by Mark T. Keating, August 24, 2005

Zebrafish fin regeneration requires the formation and maintenance of blastema cells. Blastema cells are not derived from stem cells but behave as such, because they are slow-cycling and are thought to provide rapidly proliferating daughter cells that drive regenerative outgrowth. The molecular basis of blastema formation is not understood. Here, we show that heat-shock protein 60 (*hsp60*) is required for blastema formation and maintenance. We used a chemical mutagenesis screen to identify no blastema (*nbl*), a zebrafish mutant with an early fin regeneration defect. Fin regeneration failed in *nbl* due to defective blastema formation. *nbl* also failed to regenerate hearts. Positional cloning and mutational analyses revealed that *nbl* results from a V324E missense mutation in *hsp60*. This mutation reduced *hsp60* function in binding and refolding denatured proteins. *hsp60* expression is increased during formation of blastema cells, and dysfunction leads to mitochondrial defects and apoptosis in these cells. These data indicate that *hsp60* is required for the formation and maintenance of regenerating tissue.

blastema | regeneration | zebrafish | genetics | stress response

Humans have the ability to renew lost or damaged tissues and organs. Homeostatic renewal of components of blood, skeletal muscle, and epithelia is well characterized. These constant renewal processes are believed to be mediated by the action of resident stem cells, pluripotent cells of a specific lineage. Humans also have the capacity to regenerate acutely injured tissues. Prominent among these are liver, digit-tip, and corneal regeneration. In contrast to chronic renewal, these acute regenerative processes are not mediated by the action of stem cells. Instead, they are thought to be mediated through the partial dedifferentiation and proliferation of parenchymal cells, such as hepatocytes or mesenchymal cells.

Teleost fish and urodele amphibians have remarkable regenerative capabilities. Zebrafish acutely regenerate heart (1), fins (2), optic nerve (3), scales (4) and spinal cord (5). To identify the molecular mechanisms of regeneration, we performed a genetic screen for mutant zebrafish with defects in fin and cardiac regeneration (1, 6, 7). As a result, we have begun to identify regenerative genes at specific stages of regeneration.

Zebrafish fin regeneration takes 1 week to complete at 33°C. The first step of regeneration is the closure of the wound. This is a nonproliferative event, involving the migration of existing epithelial cells to cover the wound (8). The formation of wound epidermis is completed within the first 6–12 h postamputation (hpa). The second step is blastema formation, the creation of regeneration cells that drive regeneration (8). Shortly after the wound epidermis is formed, mesenchymal cells immediately beneath this epithelium become disorganized. In urodele amphibians, this disorganizational step requires the action of matrix metalloproteinases (9). Next, a number of cells beneath the amputation plane begin to proliferate and migrate toward the wound epidermis to form a nascent blastema (8). Third, this early blastema matures to form a distal blastema consisting of slow-cycling cells that behave like stem cells even though they are derived from mesenchymal cells (8). These cells express *msxb* and *msxc*, transcriptional repressors that may help maintain a pluripotent state (8, 10, 11). These distal blastema cells are thought to give rise to proximal blastema cells that proliferate intensely and drive regenerative outgrowth (7, 8).

During regeneration, cells are exposed to a variety of stresses originating from the wound environment. Environmental stress, injury, disease, and even growth and differentiation place organisms under stress. A highly conserved cellular stress response is the induction of heat-shock proteins (Hsps), initially so-named because they were induced in *Drosophila* larvae after a slight elevation of temperature (12). Hsps are essential for cell survival in all species subjected to stress. Hsps have a chaperone function, demonstrated by their ability to bind proteins and mediate conformational changes during protein folding (13).

Hsp60 is a well characterized chaperone mainly localized in mitochondria of eukaryotic cells (14–16). Hsp60, also known as phage growth λ E large (GroEL) in bacteria, is involved in the folding and assembly of polypeptide chains into oligomeric complexes. Although Hsp60 has an essential role in the folding of many proteins, it also has additional functions (17). Interestingly, *hsp60* is up-regulated in stem cells (18) and is highly expressed in germ cells (19–21). However, it is not known whether Hsp60 is important for the function of these cells.

We performed a mutagenesis screen in zebrafish to identify temperature-sensitive mutants defective in caudal fin regeneration (6, 7). The no blastema (*nbl*) mutant showed a defect in blastema formation and maintenance in fin regeneration and failed to regenerate heart. Instead of forming an early blastema, mesenchymal cells in *nbl* did not express *msx* genes and died through apoptosis. Through positional cloning and mutational analyses, we discovered that *nbl* results from a loss-of-function missense mutation in *hsp60*. We found that *hsp60* is up-regulated in mesenchymal cells during blastema formation and that ultimately overlaps the *msxb*-positive distal blastema during regenerative outgrowth. These cells are the stem-cell-like regeneration cells required for subsequent regenerative outgrowth. Thus, *hsp60* function is required for protecting stem-cell-like regeneration cells from stress and apoptosis during regeneration.

Materials and Methods

Surgery. Fin amputation (8) and cardiac surgery were performed as described (1).

Mutagenesis and Screen for Regeneration Mutants. Mutagenesis and screen were performed as described (6).

Immunohistochemistry and *in Situ* Hybridization. Hematoxylin staining and whole-mount *in situ* hybridization were performed as

Abbreviations: Hsp, heat-shock protein; hpa, hours postamputation; dpf, days postfertilization; dpa, days postamputation; GroEL, phage growth λ E large; GroES, phage growth λ E small; LDH, lactate dehydrogenase.

†To whom correspondence may be addressed. E-mail: smakino@enders.tch.harvard.edu or mkeating@enders.tch.harvard.edu.

described (22). Antisense RNA probes were generated by using a 2.4-kb *hsp60* cDNA (EST fp49d05) and *msxb* and *msxc* sequences (11). BrdUrd incorporation assay was performed as described (8). Immunohistochemistry and acid fuchsin-orange G staining was performed as described (1, 6). To label cardiomyocytes, we used an anti-rabbit myocyte enhancer factor 2 antibody (Santa Cruz Biotechnology). Apoptotic cells were detected by using an antiactive Caspase-3 antibody (Calbiochem).

Northern Blot Analyses. Northern analyses were performed as described (6). We used Hsp60 (EST fp49d05) and β-actin cDNAs to generate probes.

Genetic Mapping and Positional Cloning. Genetic mapping and positional cloning were performed as described (6, 7). A 578-bp PCR fragment containing the mutation was amplified from *hsp60* cDNA by using the following primers: forward (Fwd), 5′-AGAGGAGTCATGATGGCCGTAG-3′ and reverse (Rev), 5′-AAGAGCAAGACCCATAGCCTCA-3′. *hsp60* genomic DNA fragment containing the mutation was amplified: Fwd, 5′-TCTCATTTAAAGGCGTAGTTCACAG-3′ and Rev, 5′-CCTTAATGACGGCCACTCCATCTGA-3′. The GenBank accession number for *hsp60* is NM_181330.

EM. EM was performed as described (6).

Phenotype Rescue and Morpholino Antisense Knockdown. WT *hsp60* cDNA or mutated *hsp60* cDNA (V324E) was subcloned into the pCS2+ expression vector (23). Rescue experiments were performed as described (6). Antisense morpholino oligonucleotides against *hsp60* 5′-CATGACACTGGGTAAACGCAGCATT-3′ (Gene Tools, Carvalis, OR) were injected at 300 μM into one-cell-stage WT embryos and screened at 3 days postfertilization (dpf) for the *hsp60* phenotype.

***In Vitro* Functional Assay.** The mutant GroEL V300E was constructed by using the QuikChange site-directed mutagenesis kit (Stratagene). WT GroEL, phage growth λ E small (GroES), and GroEL V300E proteins were purified as described (24). *In vitro* functional assay were performed as described (24, 25).

Statistics. BrdUrd-positive nuclei were counted, and results were expressed as mean ± SEM. Statistical significance determined through two-tailed Student's *t* test.

Results

Genetic Screen for Regeneration Mutants and Identification of *nbl*. To identify mutants that failed to regenerate, we treated male zebrafish with *N*-ethyl-*N*-nitrosourea and generated mutagenized families by early pressure parthenogenesis (6, 7). We assumed that many regeneration genes would also be required for development, so we screened for temperature-sensitive mutants. We raised 431 families to adulthood at 25°C, amputated caudal fins, and shifted the temperature to 33°C for 7 days before assessing regeneration. Of note, WT fin regeneration is completed normally at 33°C and proceeds approximately two times faster than at 25°C (2). To enhance the specificity of our screen, we selected for fish that survived the restrictive condition (33°C) for at least 2 weeks. To increase the likelihood of identifying genes critical for the early phases of regeneration, we selected for fish that failed to express *msxb*, a marker of early blastema formation. Through these processes, we identified *nbl*, a temperature-sensitive zebrafish fin regeneration mutant.

The *nbl* phenotype was inherited as a recessive trait and was identified in a family in which 4 of 17 members displayed regenerative defects. *nbl* regenerates did not form new bone and failed to grow beyond the amputation plane after 7 days at 33°C (Fig. 1*A*). *nbl* regenerated fins at the permissive temperature, 25°C.

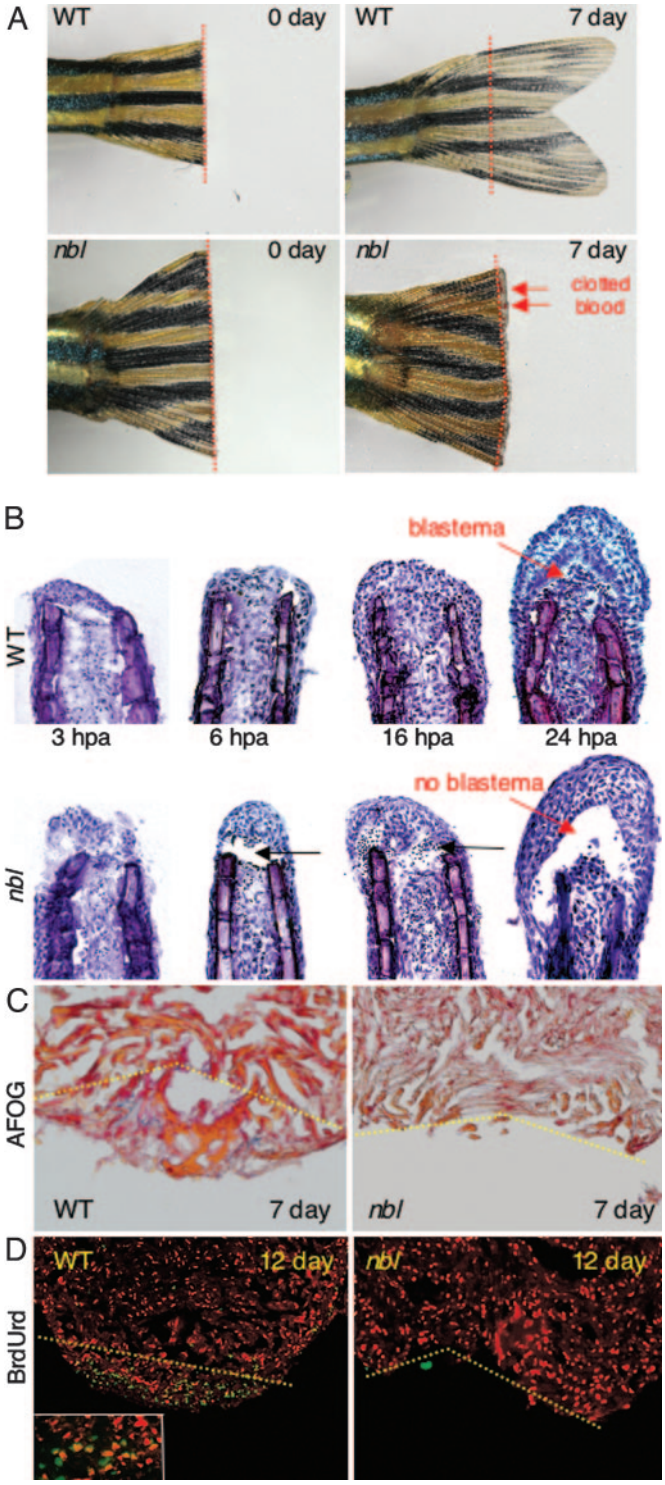

Fig. 1. *nbl*, a temperature-sensitive regeneration mutant. (*A*) Whole-mount WT and *nbl* caudal fin regenerates at 0 and 7 dpa. *nbl* shows a clear block in fin regeneration. Red dashed lines demarcate amputation plane. Red arrows show clotted blood in *nbl*. (*B*) Sections of regenerating fins stained with hematoxylin at 3, 6, 16, and 24 hpa (33°C). A fluid- or bloodfilled space separates the wound epidermis from mesenchyme in *nbl* (black arrow). *nbl* fins fail to form blastema (red arrow; 24 hpa). (*C*) Heart sections 7 dpa stained with acid fuchsin-orange G to stain fibrin (orange) and collagen (blue) deposits. *nbl* ventricle did not initiate cardiac regeneration. Yellow dashed line demarcates the amputation plane. (*D*) Heart regeneration at 12 dpa. Myocyte enhancer factor 2 staining marks cardiomyocytes (red), and BrdUrd (green) identifies cycling cells. A low percentage of cardiomyocytes incoporate BrdUrd (orange) in WT. No evidence of myocyte or nonmyocyte proliferation was observed in *nbl* hearts.

To further define the *nbl* regeneration defect, we performed histologic analyses on fin regenerates obtained from sequential stages of regeneration at 33°C. Wound healing appeared normal (Fig. 1*B*). However, a fluid- or bloodfilled space separated the wound epidermis from mesenchyme in *nbl* mutant as early as 6 hpa (Fig. 1*B*). Occasionally, this space was filled by collapsing wound epidermis. This phenotypic abnormality was more pronounced at 24 hpa, at which point WT zebrafish form the initial blastema. In contrast, *nbl* regenerates developed large acellular areas where the blastema is normally formed (Fig. 1*B*). The name *nbl* was derived from this no blastema phenotype.

To determine whether *nbl* was essential for cardiac regeneration, we surgically removed ≈20% of the ventricular myocardium from 1-year-old adults and examined hearts histologically. WT fish formed fibrin clots by 7 days postamputation (dpa; Fig. 1*C*), and cardiac myofibers penetrated the clot and constructed a new muscle around the wound by 17 days (1). The restoration of cardiac muscle resulted from cardiomyocyte proliferation (1) (Fig. 1*D*). In contrast, *nbl* could not initiate cardiac regeneration. *nbl* failed to fill in the wound area with fibrin clots or collagen scar (Fig. 1*C*, $n = 10$). BrdUrd studies showed no evidence of myocyte or nonmyocyte proliferation around the wound at 12 dpa (Fig. 1*D*, $n = 5$).

Blastema Defects in *nbl*. To determine the cellular mechanism of the *nbl* regenerative failure, we examined the histology of *nbl* fin regenerates. During blastema formation (24 hpa) *msxb* is expressed among mesenchymal cells that ultimately form the blastema (Fig. 2*A*). In contrast to WT, *msxb* expression was absent in *nbl* and there was no evidence of blastema formation (Fig. 2*A*).

To further dissect blastema formation in *nbl*, we assessed the proliferation of mesenchymal cells by using BrdUrd incorporation (Fig. 2*B*). BrdUrd is a thymidine analog that is incorporated into DNA during replication. Interestingly, the proliferation level of mesenchyme tissue proximal to the amputation plane was slightly increased in *nbl* regenerates (Fig. 2*B*; WT 46.2 ± 4.0%, *nbl* 62.6 ± 3.4%, $P = 0.0086$, $n = 7$). Proliferation of epidermal cells in *nbl* regenerates did not differ from WT (Fig. 2*B*). However, the lack of mesenchymal cells above the amputation plane in *nbl* is further evidence for failed blastema formation (Fig. 2*B*).

To determine whether programmed cell death accounted for lost tissue in *nbl* mutants, WT and *nbl* fish were allowed to regenerate for 16 hpa at 25°C before a 4-h incubation at the restrictive temperature of 33°C. We detected a small number of active Caspase-3-positive cells in the mesenchyme beneath the wound epidermis, where mesenchymal disorganization occurs (Fig. 2*C*). These data indicate that a small number of cells in the region of blastema formation undergo apoptosis in *nbl*.

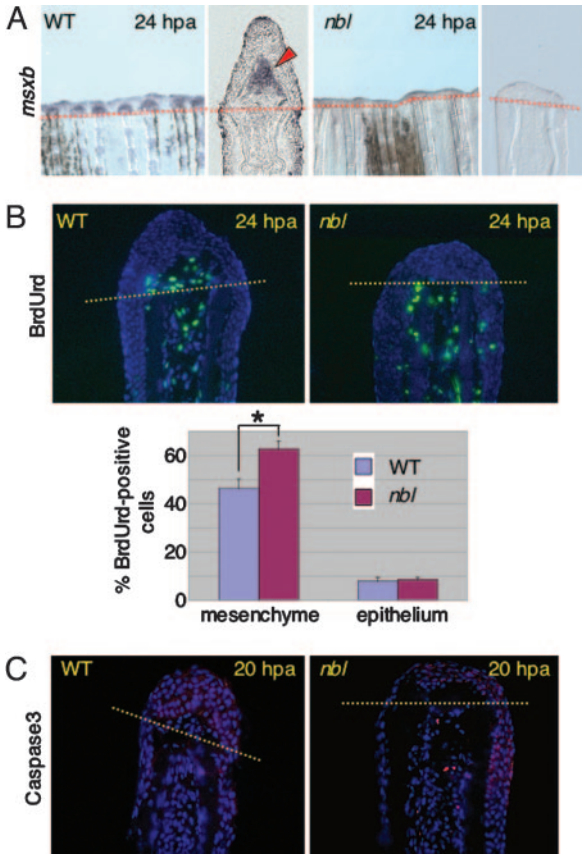

Fig. 2. Failed blastema formation in *nbl*. (*A*) Whole-mount *in situ* hybridization and longitudinal sections of *msxb* in WT and *nbl* fin regenerates at 24 hpa. *msxb* (red arrowhead) marks early blastema cells. Note the absence of *msxb* expression in *nbl*, indicating failure of early blastema formation. (*B*) Sections from WT and *nbl* regenerates immunostained for BrdUrd (green) and DAPI (blue). Fish were treated with BrdUrd for 6 h before harvesting at 24 hpa. No blastema is observed in *nbl* regenerates at 33°C. However, mesenchymal cell proliferation in *nbl* is slightly increased. Epidermal cell proliferation in *nbl* is comparable to WT at 33°C. Data in graph are the mean ± SEM; $n = 7$; *, $P < 0.01$. (*C*) Sections from WT and *nbl* regenerates immunostained for active Caspase-3 (red) and DAPI (blue). WT and *nbl* fish regenerated for 16 h at 25°C followed by a 4-h incubation at 33°C. Note there are Caspase-3-positive cells proximal to the amputation plane in *nbl*. Normally, this is where mesenchymal tissue disorganization occurs, a process that immediately precedes early blastema formation.

Distal Blastema Defects in *nbl*. The blastema in regenerating zebrafish fins consists of two compartments, the distal and proximal blastemas. The distal blastema is a small number of *msxb*-positive cells immediately beneath the wound epidermis (8). Although derived from mesenchymal cells during blastema formation, these distal blastema cells behave like stem cells, because they are slow-cycling and are thought to give rise to proximal blastema cells (8). In contrast, proximal blastema cells do not express *msxb* and proliferate intensely (7, 8). To determine the effect of the *nbl* mutation on the mature blastema during regenerative outgrowth (beyond 48 hpa at 33°C), we performed temperature-shift experiments. WT and *nbl* fish were allowed to regenerate for 5 days at 25°C before an 8-h incubation at 33°C. The temperature shift led to a loss of *msxb* expression in *nbl* distal blastema cells (Fig. 3*A*, $n = 15$). However, in WT regenerates, *msxb* expression was maintained (Fig. 3*A*). This observation was confirmed by using other distal blastema markers, including *msxc* (data not shown).

During regenerative outgrowth, the proximal blastema cells proliferate intensely. To determine the effect of *nbl* on cell proliferation, fish were treated with BrdUrd during the final 2 h of the 8 h incubation at 33°C. Mesenchymal and epidermal cell proliferation in *nbl* fish were unaffected during regenerative outgrowth. However, distal blastemal cells were absent in *nbl* mutants after the brief heat shock (Fig. 3*B*; red arrowhead).

To determine whether apoptosis accounted for the absent distal blastema cells in *nbl*, we examined active Caspase-3 immunostaining. After a 4-hour heat shock, we identified activated Caspase-3 staining in the distal blastema (Fig. 3*C*). These data demonstrate that *nbl* is required for the survival and maintenance of *msxb*-positive distal blastema cells.

To determine the subcellular defect in *nbl*, we examined distal blastema cells of WT and *nbl* regenerates using EM. WT distal blastema cells had large nuclei with pronounced nucleoli, abundant ribosomes, rough endoplasmic reticulum, and clusters of mitochondria (Fig. 3*D*). The presence of apoptotic cells was detected after 4-h incubation at 33°C in *nbl* regenerates (data not shown). After 8 h at 33°C, *nbl* distal blastema cells showed dilated mitochondria with empty matrix (Fig. 3*D*). Of note, *nbl* mitochondrial shape was normal in regions other than the distal blastema (data not shown).

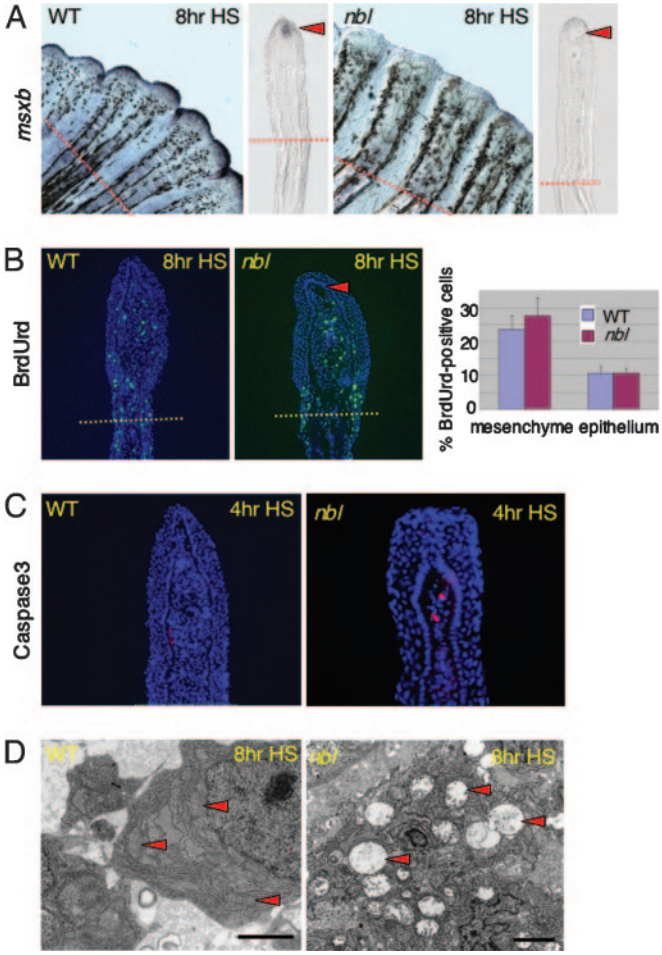

Fig. 3. Failed blastema maintenance in *nbl*. (*A*) Whole-mount *in situ* hybridization of *msxb* in WT and *nbl* fin regenerates. Fish were incubated for 5 days at 25°C before an 8-h incubation at 33°C. *msxb* expresson is absent in the *nbl* distal blastema (red arrowhead). (*B*) Sections of WT and *nbl* regenerates immunostained for BrdUrd (green) and DAPI (blue). Fish were incubated with BrdUrd during the final 2 h at 33°C. Note that an 8-h incubation at 33°C does not affect mesenchymal and epidermal cell proliferation levels during regenerative outgrowth but distal blastemal cells disappear in *nbl* (red arrowhead). (*C*) Apoptosis of blastema cells in *nbl*. WT and *nbl* fish regenerated for 5 days at 25°C followed by 4 h at 33°C. Fins were immunostained with active Caspase-3 (red) and DAPI (blue). Note that distal blastema cells undergo apoptosis in *nbl*. (*D*) Electron micrographs of distal blastema in WT and *nbl* fish. Fins regenerated for 5 days at 25°C followed by 8-h incubations at 33°C. Note the larger mitochondria with empty matrix (red arrowhead) in *nbl* mutants. (Bars, 2 μm.)

These data indicate that the *nbl* mutation causes dilated mitochondria and apoptosis selectively in distal blastema cells.

Hsp60 Is the *nbl* Gene. To define the *nbl* gene, we scored 2,302 fish from *nbl* × *nbl*/+ mapping crosses for regeneration defects. Initial genotypic mapping placed *nbl* between z54324 and z50394 on chromosome 9. To refine localization of *nbl*, we initiated a chromosomal walk using bacterial artificial chromosome clones from z54324 and z7144, which flanked the 0.61-cM *nbl* region (Fig. 4*A*). Single-strand conformation polymorphism markers from the z06z013214 and zC117M22z genomic clones confined *nbl* to a 0.13-cM critical region (Fig. 4*A*). Three markers, fi27b05, fi98e03, and zK31k6tA1, were nonrecombinant (Fig. 4*A*).

Four transcripts were identified in the *nbl* critical region: *hsp60*, *hsp10*, *preimplantation protein 3*, and *322240M22 Rik protein*. DNA sequence analysis of *hsp10*, *preimplantation protein 3*, and

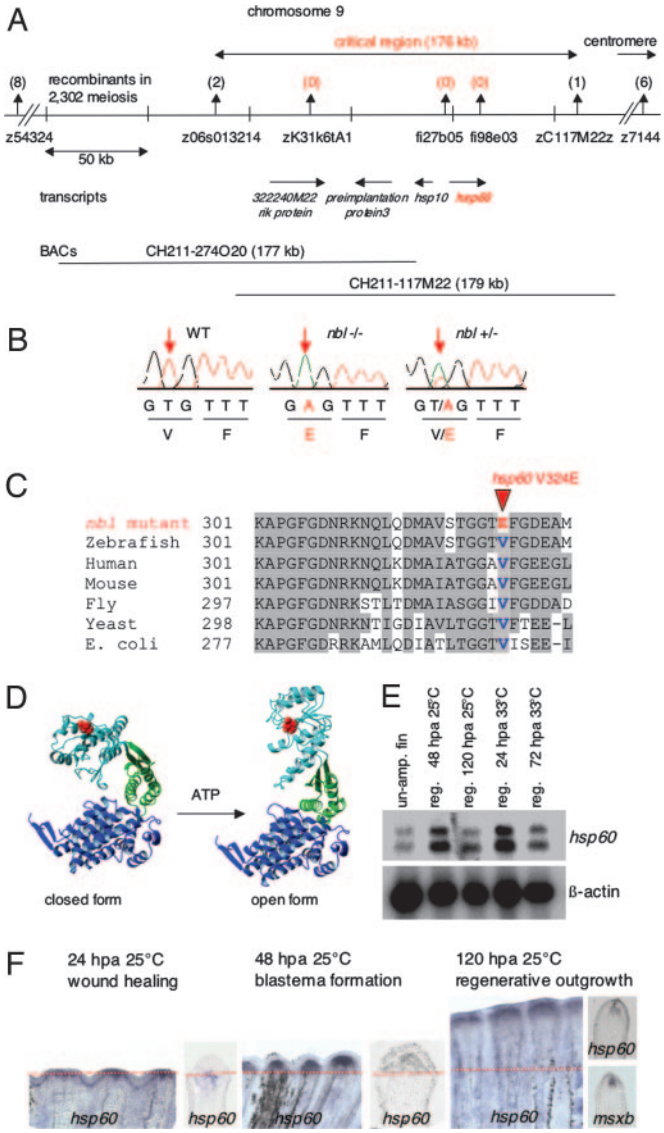

Fig. 4. *hsp60* is the *nbl* gene. (*A*) Genetic and physical map of *nbl*. Linkage map (*Top*), transcripts (*Middle*), and physical map (*Bottom*) places *nbl* between z54324 and z7144. Numbers in parentheses show recombination events from 2,302 meioses between *nbl* phenotype and linked genetic markers. (*B*) DNA sequence analysis from *nbl* and WT strains revealed a unique thymidine to adenosine mutation in *nbl*, causing valine-324 to glutamic acid missense mutation in Hsp60 (red arrows). (*C*) Multiple species alignment of the *hsp60* region containing the V324E mutation. Note complete conservation of valine-324 among species, including *E. coli*. (*D*) Ribbon drawing structure of one subunit in the *cis* GroEL (Hsp60) ring. Figures were generated by using MOLMOL (32) and coordinates from Protein Data Bank file 1AON (33). The location of the mutation site is shown in red space-filling form in the apical domain (light blue). Intermediate (green) and equatorial domains (blue) are also shown. (*E*) Northern blot analysis of *hsp60* expression in regenerating caudal fin. *hsp60* levels are up-regulated during blastema formation at both 25°C and 33°C. β-actin expression shown as a control. (*F*) Whole-mount *in situ* hybridization of *hsp60* during regeneration. Fish were incubated at 25°C to ensure expression is not induced by heat-shock treatment. *hsp60* expression is first induced beneath the wound epidermis, where mesenchymal tissue disorganization occurs at 24 hpa. At 48 hpa, *hsp60* is expressed in the newly formed blastema. At 120 hpa, *hsp60* expression is up-regulated in the distal blastema where *msxb* is expressed.

322240M22 Rik protein failed to reveal mutations (data not shown). DNA sequence analysis of cDNAs from *nbl*, and several WT strains revealed a thymidine to adenosine mutation in *hsp60* (Fig. 4*B*),

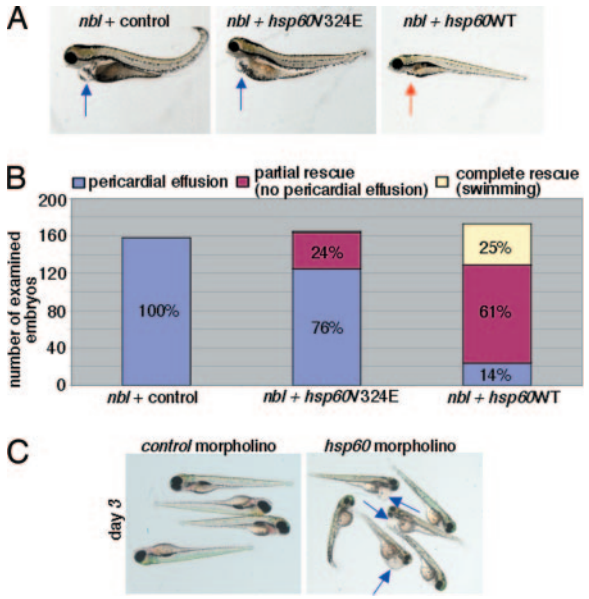

Fig. 5. *hsp60* rescues *nbl*. (*A*) *nbl* embryos raised at 33°C develop pericardial effusion and die at 5 dpf. Embryos from homozygous *nbl* crosses were injected with 1 nl of 200 ng/μl mRNA (*hsp60*WT, *hsp60*V324E, or enhanced GFP) and then transferred to 33°C. Blue arrows mark pericardial effusion; red arrow shows normal cardiac anatomy. Note that *hsp60*WT mRNA rescues the pericardial effusion phenotype. (*B*) *nbl* embryos were scored for the presence of pericardial effusion and ability to swim at 5 dpf. *Hsp60*WT mRNA rescues the *nbl* phenotype. (*C*) WT embryos injected with morpholino against *hsp60* show pericardial effusion at 3 dpf at 28.5°C. Blue arrows mark pericardial effusion. These results indicate that *hsp60* dysfunction, and not heat shock, caused the *nbl* phenotype.

causing a valine-324 to glutamic acid substitution. Multiple species alignment of *hsp60* showed complete conservation of valine-324 among species, including *Escherichia coli* (Fig. 4*C*). A ribbon diagram showing the structure of GroEL (*E. coli* homolog of Hsp60) showed that the analogous valine (red) is located in the apical domain (light blue; Fig. 4*D*). This apical domain is important for Hsp10 and nonnative protein binding (24).

To define the timing and localization of *hsp60* expression during fin regeneration and to determine whether *hsp60* expression is consistent with the *nbl* phenotype, we performed Northern blot and *in situ* hybridization analyses. Fish were incubated at 25°C to ensure that expression was not induced by heat-shock treatment. We found that zebrafish *hsp60* was expressed in all adult somatic tissues examined, including unamputated caudal fins. The highest expression was detected in testis and ovary (data not shown). The level of *hsp60* mRNA in the unamputated caudal fin was low (Fig. 4*E*). However, *hsp60* was up-regulated during blastema formation (48 hpa at 25°C, 24 hpa at 33°C; Fig. 4*E*). The high level of *hsp60* expression declined to levels similar to unamputated fins during subsequent stages of regeneration (Fig. 4*E*). *In situ* hybridization analyses revealed that *hsp60* expression was first observed at 12 hpa at 25°C (data not shown). At 12 and 24 hpa, *hsp60* was localized to the mesenchymal cells immediately beneath the wound epidermis (Fig. 4*F*). These cells demarcate the region undergoing tissue disorganization. At this timepoint, the cell proliferation, which ultimately forms the rudimentary blastema, had not yet begun (8). Thus, *hsp60* expression is up-regulated before blastema formation.

Later, when the rudimentary blastema is formed (48 hpa at 25°C), *hsp60* was highly expressed in blastemal cells (Fig. 4*F*). *hsp60* expression was overlapped with *msxb*, a blastemal marker. During regenerative outgrowth (120 hpa at 25°C), *hsp60* expression was up-regulated in the distal blastema (Fig. 4*F*). These data indicate that *hsp60* is up-regulated in *msxb*-positive blastema cells during fin regeneration, and *hsp60* expression patterns are consistent with the *nbl* phenotype.

Rescue of *nbl* by Overexpression of Hsp60. To determine whether *hsp60* was essential for embryonic development, we raised embryos at 33°C. Although 81% (97/120) of WT or heterozygous zebrafish reached the swimming stage, no *nbl* mutants attained this stage at 33°C. *nbl* defects included cardiac hypertrophy and progressive pericardial effusion (data not shown). *nbl* fish raised at 25°C appeared to grow normally, because 87% (515/593) of *nbl* mutants survived to adulthood.

To confirm that *hsp60* was the *nbl* gene, we injected mRNA encoding either WT or mutant (V324E) *hsp60* transcripts into *nbl* embryos. After injection, embryos were transferred to 33°C. We scored for ability to swim and for pericardial effusion, because *nbl* embryos consistently demonstrated pericardial effusion at 33°C (536/536; Fig. 5*A*). *nbl* embryos injected with the enhanced GFP control showed pericardial effusion (158/158) and did not reach the swimming stage (0/158; Fig. 5*B*). In contrast, 25% (44/173) of *nbl* embryos injected with WT *hsp60* mRNA were able to swim, and 86% (149/173) did not display the *nbl* pericardial effusion phenotype (Fig. 5 *A* and *B*). We conclude that WT *hsp60* overexpression rescues *nbl* mutants from embryonic lethality.

To determine whether the embryonic pericardial effusion resulted specifically from *hsp60* dysfunction rather than heat shock, we injected WT embryos with *hsp60* morpholinos. Most (74%; 189/255) of these embryos showed pericardial effusion at 28.5°C (Fig. 5*C*). These data indicate that Hsp60 dysfunction, and not heat shock, caused the *nbl* phenotype. Taken together, our linkage, mutation, expression, mRNA rescue and morpholino data all indicate that *hsp60* is the *nbl* gene.

Functional Consequences of the *nbl* Mutation. Hsp60 is a molecular chaperone that prevents misfolding and promotes refolding of nonnative proteins (15). This protein is a member of the highly conserved family of molecular chaperones which includes GroEL,

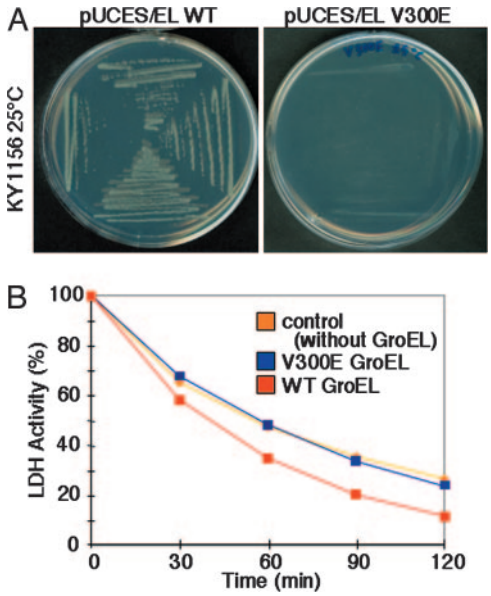

Fig. 6. GroEL V300E causes reduced chaperone function. (*A*) The *E. coli* strain KY1156 (26) requires functional GroEL for growth. GroEL V300E is analogous to Hsp60 V324E. KY1156 transfected with GroEL V300E decreased growth at 25°C, suggesting this mutation reduces GroEL function. (*B*) GroEL V300E shows decreased affinity for nonnative form of LDH. LDH activity was measured after addition of nonpermissive solution (without ATP at 42°C) at time 0 in the presence of mutant (blue) or WT GroEL (red). Negative control was without GroEL (orange).

the *E. coli* homolog of Hsp60. Hsp60 depends upon its cochaperone, Hsp10 (GroES in *E. coli*). Before GroEL binds ATP and GroES, the nonnative protein is held simultaneously by multiple GroEL apical domains (Fig. 4*D*; light blue).

To determine whether Hsp60 function was affected by the V324E mutation, we evaluated the analogous mutation (V300E) in GroEL in a bacterial growth assay using *E. coli* strain KY1156, which requires functional GroEL for growth (26). We transformed KY1156 cells with a plasmid that produces WT GroES and GroEL V300E. As a control, we also transformed KY1156 cells with WT GroES and WT GroEL. At 25°C, growth of the mutant transformed colonies was extremely slow (Fig. 6*A*), suggesting that insufficient quantities of functional GroEL protein was present. These data indicate that at 25°C, GroEL V300E was not able to function as a replacement for WT GroEL. These data suggest that GroEL V300E is a loss-of-function mutation.

To perform chaperone function, GroEL must bind nonnative proteins. Lactate dehydrogenase (LDH) activity was measured following addition of nonpermissive solution (without ATP at 42°C) at time 0 in the presence of mutant or WT GroEL. WT GroEL binds nonnative LDH, which changed the equilibrium between native and nonnative LDH in solution. This binding, in turn, drove the equilibrium to lower native and increased nonnative LDH, thus lowering LDH activity. GroEL V300E did not lower LDH activity, similar to the control (without GroEL). These data suggest that GroEL V300E has lower binding affinity for the nonnative form of LDH at 42°C (Fig. 6*B*).

Discussion

In this study, we used a genetic approach to study regeneration with a mutagenesis screen for zebrafish fin regeneration mutants. We identified the *nbl* mutant, which displayed a defect in blastema formation and maintenance. The *nbl* defect was caused by a mutation in *hsp60*. Evidence indicating that *hsp60* is the *nbl* gene include: (*i*) genetic linkage of *nbl* to a 0.13-cM region containing *hsp60*, (*ii*) absence of mutations in other genes within the critical region, (*iii*) identification of a V324E substitution in a conserved amino acid in Hsp60, (*iv*) absence of this mutation in all common zebrafish strains, (*v*) rescue of *nbl* embryonic lethality by *hsp60* mRNA, (*vi*) *hsp60* expression consistent with the *nbl* phenotype, and (*vii*) *hsp60* morpholino phenocopies the *nbl* embryonic phenotype.

Our data indicate that *hsp60* expression is up-regulated in blastema cells during zebrafish fin regeneration, and that Hsp60 function is required for blastema formation and viability. In previous studies, we have demonstrated that distal blastema cells behave like stem cells (8). Perhaps Hsp60 has a unique role in pluripotent cells. Interestingly, other studies have demonstrated that stem cells exhibit increased Hsp expression (18). Additionally, during rat spermatogenesis, Hsp60 is expressed in spermatogonia and early spermatocytes but not in postmeiotic germ cells (19–21). Furthermore, knockdown of *hsp60* in *Caenorhabditis elegans* showed a sterile phenotype (27), indicating that Hsp60 is required for gametogenesis. It is possible that blastema cells are under increased stress because of their unique niche and proximity to highly proliferative cells, which make them sensitive to Hsp60 dysfunction. Alternatively, blastema cells may have increased sensitivity to normal or even low levels of stress due to the importance of high fidelity in stem cells.

nbl mutants show an early and complete regeneration block in both fin and heart. It is difficult to conclude that these phenotypes are caused solely by reduced chaperone function. A possible explanation is that Hsp60 is the latest addition to the growing list of Toll-like receptor ligands (17, 28–30). It is tempting to consider Toll-like receptors as a general danger signal receptors (31) involved in tissue repair. Trauma triggers an immunogenic environment, and Hsp60 may play a vital role in these processes.

In summary, we have discovered that Hsp60 is required for blastema formation and maintenance during fin regeneration. These findings suggest that Hsp60 may play a role in undifferentiated cells.

We thank K. Poss and A. Nechiporuk for protocols, advice, and helpful suggestions; A. Hillam, L. Wilson, A. Sanchez, C. Richards, and O. Paugois for fish care; H. Mulhern for the EM; W. Zhu for genotyping; L. Zon, S. Odelberg, E. Kaji, I. Splawski, F. Engel, M. Schebesta, and K. Tseng for critique of the manuscript; and Keating laboratory members for helpful discussions. This work was supported by National Heart, Lung, and Blood Institute Grant SCCOR RFA HL 02-027; the Uehara Memorial Foundation; and the Donald W. Reynolds Foundation.

1. Poss, K. D., Wilson, L. G. & Keating, M. T. (2002) *Science* **298,** 2188–2190.
2. Johnson, S. L. & Weston, J. A. (1995) *Genetics* **141,** 1583–1595.
3. Bernhardt, R. R., Tongiorgi, E., Anzini, P. & Schachner, M. (1996) *J. Comp. Neurol.* **376,** 253–264.
4. Bereiter-Hahn, J. & Zylberberg, L. (1993) *Comp. Biochem. Physiol.* **105A,** 625–641.
5. Becker, T., Wullimann, M. F., Becker, C. G., Bernhardt, R. R. & Schachner, M. (1997) *J. Comp. Neurol.* **377,** 577–595.
6. Nechiporuk, A., Poss, K. D., Johnson, S. L. & Keating, M. T. (2003) *Dev. Biol.* **258,** 291–306.
7. Poss, K. D., Nechiporuk, A., Hillam, A. M., Johnson, S. L. & Keating, M. T. (2002) *Development (Cambridge, U.K.)* **129,** 5141–5149.
8. Nechiporuk, A. & Keating, M. T. (2002) *Development (Cambridge, U.K.)* **129,** 2607–2617.
9. Vinarsky, V., Atkinson, D. L., Stevenson, T. J., Keating, M. T. & Odelberg, S. J. (2005) *Dev. Biol.* **279,** 86–98.
10. Odelberg, S. J., Kollhoff, A. & Keating, M. T. (2000) *Cell* **103,** 1099–1109.
11. Akimenko, M. A., Johnson, S. L., Westerfield, M. & Ekker, M. (1995) *Development (Cambridge, U.K.)* **121,** 347–357.
12. Ashburner, M. & Bonner, J. J. (1979) *Cell* **17,** 241–254.
13. Rye, H. S., Roseman, A. M., Chen, S., Furtak, K., Fenton, W. A., Saibil, H. R. & Horwich, A. L. (1999) *Cell* **97,** 325–338.
14. Cheng, M. Y., Hartl, F. U., Martin, J., Pollock, R. A., Kalousek, F., Neupert, W., Hallberg, E. M., Hallberg, R. L. & Horwich, A. L. (1989) *Nature* **337,** 620–625.
15. Martin, J., Horwich, A. L. & Hartl, F. U. (1992) *Science* **258,** 995–998.
16. Soltys, B. J. & Gupta, R. S. (1996) *Exp. Cell Res.* **222,** 16–27.
17. Ohashi, K., Burkart, V., Flohe, S. & Kolb, H. (2000) *J. Immunol.* **164,** 558–561.
18. Ramalho-Santos, M., Yoon, S., Matsuzaki, Y., Mulligan, R. C. & Melton, D. A. (2002) *Science* **298,** 597–600.
19. Paranko, J., Seitz, J. & Meinhardt, A. (1996) *Differentiation* **60,** 159–167.
20. Sarge, K. D. & Cullen, K. E. (1997) *Cell Mol. Life Sci.* **53,** 191–197.
21. Werner, A., Meinhardt, A., Seitz, J. & Bergmann, M. (1997) *Cell Tissue Res.* **288,** 539–544.
22. Poss, K. D., Shen, J., Nechiporuk, A., McMahon, G., Thisse, B., Thisse, C. & Keating, M. T. (2000) *Dev. Biol.* **222,** 347–358.
23. Turner, D. L. & Weintraub, H. (1994) *Genes Dev.* **8,** 1434–1447.
24. Kawata, Y., Kawagoe, M., Hongo, K., Miyazaki, T., Higurashi, T., Mizobata, T. & Nagai, J. (1999) *Biochemistry* **38,** 15731–15740.
25. Kawata, Y., Nosaka, K., Hongo, K., Mizobata, T. & Nagai, J. (1994) *FEBS Lett* **345,** 229–232.
26. Miyazaki, T., Yoshimi, T., Furutsu, Y., Hongo, K., Mizobata, T., Kanemori, M. & Kawata, Y. (2002) *J. Biol. Chem.* **277,** 50621–50628.
27. Rual, J. F., Ceron, J., Koreth, J., Hao, T., Nicot, A. S., Hirozane-Kishikawa, T., Vandenhaute, J., Orkin, S. H., Hill, D. E., van den Heuvel, S., *et al.* (2004) *Genome Res.* **14,** 2162–2168.
28. Lemaitre, B., Nicolas, E., Michaut, L., Reichhart, J. M. & Hoffmann, J. A. (1996) *Cell* **86,** 973–983.
29. Vabulas, R. M., Ahmad-Nejad, P., da Costa, C., Miethke, T., Kirschning, C. J., Hacker, H. & Wagner, H. (2001) *J. Biol. Chem.* **276,** 31332–31339.
30. Medzhitov, R., Preston-Hurlburt, P. & Janeway, C. A., Jr. (1997) *Nature* **388,** 394–397.
31. Matzinger, P. (2002) *Science* **296,** 301–305.
32. Koradi, R., Billeter, M. & Wuthrich, K. (1996) *J. Mol. Graphics* **14,** 29–32, 51–55.
33. Xu, Z., Horwich, A. L. & Sigler, P. B. (1997) *Nature* **388,** 741–750.